The Ordovician strata of the Ennedi Plateau, northeastern Chad (Erdi Basin)

Jean-François Ghienne, Abderamane Moussa, Abakar Saad, Barnabé Djatibeye, Hissein Mahamat Youssouf

The Ordovician strata of the Ennedi Plateau, northeastern Chad (Erdi Basin)
Les grès ordoviciens du plateau de l'Ennedi, NE du Tchad (Bassin des Erdis)

Ghienne Jean-François, Moussa Abderamane, Saad Abakar, Djatibeye Barnabé, Youssouf Hisseini Mahamat

Note pour les *Comptes Rendus – Géosciences*, acceptée le 2 novembre 2022.

Abstract. In the Ennedi (NE Chad), Cambrian(?)-Ordovician to Carboniferous strata represent one of the most proximal succession of the north-facing Gondwana platform. This study presents preliminary results related to the *c.* 200 m-thick Lower Sandstones and overlying Bedo Formation, which essentially record Early to Middle Ordovician flooding events and the end-Ordovician glaciation and subsequent deglaciation. In the Lower Sandstones, fluvial-dominated deposits (prevailing cross-stratification, NW to NNE paleocurrent trends) include intervening high-frequency marine incursions (tidal deposits, ichnofacies including *Cruziana* and *Arthrophycus).* Above an erosional unconformity, the end-Ordovician glacial record consists of fluvioglacial conglomeratic deposits atop the Lower Sandstones, which are in turn superimposed by the fine-grained Bedo Formation. The latter interval, onlapping an exhumed erosion surface showing north-trending km-scale glacial lineations, shows glaciomarine deposits only at its base and possibly include Lower Silurian deposits in its upper part.

Résumé. Dans le massif de l'Ennedi, au NE du Tchad, les dépôts s'étageant du Cambrien(?)-Ordovicien au Carbonifère représentent l'une des successions les plus proximales de la plate-forme 'nord-gondwanienne'. Cette étude présente quelques résultats préliminaires sur les Grès Inférieurs, épais d'environ 200 m, et la Formation de Bedo sus-jacente. Cet intervalle stratigraphique enregistre essentiellement les événements transgressifs de l'Ordovicien inférieur à moyen, puis la glaciation, ainsi que la déglaciation consécutive, de la fin de l'Ordovicien. Dans les Grès Inférieurs, les dépôts à dominante fluviatile (dominance des faciès à laminations obliques, orientation des courants dans un secteur NW à NNE) comprennent des incursions marines à haute fréquence (dépôts de marée, ichnofaciès à *Cruziana* et *Arthrophycus*). Au-dessus d'une discordance d'érosion venant tronquer les Grès Inférieurs, la succession glaciaire débute avec des dépôts conglomératiques fluvioglaciaires et termine avec une unité à dominante argileuse (Formation de Bedo). Cette dernière, qui scelle une surface d'érosion exhumée à linéations glaciaires orientées vers le nord et d'échelle kilométrique, montre des dépôts glaciomarins uniquement à sa base. Elle pourrait inclure dans sa partie sommitale des dépôts du Silurien inférieur.

The Ordovician strata of the Ennedi Plateau, northeastern Chad (Erdi Basin)

Ghienne[a*] Jean-François, Moussa[b] Abderamane, Saad[b] Abakar, Djatibeye[b] Barnabé, Youssouf[c] Hisseini Mahamat

[a] Institut Terre et Environnement de Strasbourg, UMR7063, CNRS – Université de Strasbourg, 5, rue R. Descartes, 67000 Strasbourg, France. ghienne@unistra.fr
[b] Laboratoire Hydro-Géosciences and Réservoirs, Département de Géologie et Paléontologie, Université de N'Djamena, BP 1027, N'Djamena, Chad. mellah03@yahoo.fr, saabakar8@gmail.com, barnabdjatibeye24@yahoo.com
[c] Ministère du Pétrole du Chad, N'Djamena, Chad. youssoufhisseini@gmail.com

Abstract. In the Ennedi (NE Chad), Cambrian(?)-Ordovician to Carboniferous strata represent one of the most proximal succession of the north-facing Gondwana platform. This study presents preliminary results related to the *c.* 200 m-thick Lower Sandstones and overlying Bedo Formation, which essentially record Early to Middle Ordovician flooding events and the end-Ordovician glaciation and subsequent deglaciation. In the Lower Sandstones, fluvial-dominated deposits (prevailing cross-stratification, NW to NNE paleocurrent trends) include intervening high-frequency marine incursions (tidal deposits, ichnofacies including *Cruziana* and *Arthrophycus).* Above an erosional unconformity, the end-Ordovician glacial record consists of fluvioglacial conglomeratic deposits atop the Lower Sandstones, which are in turn superimposed by the fine-grained Bedo Formation. The latter interval, onlapping an exhumed erosion surface showing north-trending km-scale glacial lineations, shows glaciomarine deposits only at its base and possibly include Lower Silurian deposits in its upper part.

1. Introduction

The Ennedi is a sandstone plateau in northeastern Chad (Fig. 1), which exposes a Palaeozoic succession expanding from the Cambrian(?)-Ordovician to the Carboniferous. The succession characterizes one of the innermost segments of the wide, north-facing Gondwana platform that once extended from northern South America to the Middle East. Stratigraphic archives of such a proximal segment of the platform remain largely understudied today (Klitzsch, 1994).

Pioneering work occurred at the beginning of the 20th century (Denaeyer, 1924; Fritel, 1924, with revision by Lemoigne et al., 1992; Lacroix and Tilho, 1919; Sandford, 1935). Soon after the Second World War, French geologists of the Borkou-Ennedi-Tibesti mapping project (Bizard et al., 1955; Bonnet et al., 1955; Lessertisseur, 1956; Wacrenier, 1958) recognized that the Palaeozoic of northern Chad is largely comparable to the stratigraphy established by Kilian (1924) for the Central Sahara. The latter comprises fundamentally two geomorphic units: the Cambrian-Ordovician Lower Sandstones resting unconformably on a Panafrican (Proterozoic-earliest Cambrian) basement, and the Silurian-Devonian Upper Sandstones. The two units are separated from each other by the intra-Tassilian Trough that, in Algeria and western Libya, includes the lower Silurian graptolitic shales (e.g. the Tanezzuft shales of the Murzuq Basin, Bellini and Massa, 1980). Publications by German geologists

provided details about facies and ichnofacies associations, stratigraphical ages and regional correlation schemes (Klitzsch, 1965, 1966, 1968, 1970; Seilacher, 1970, see also Seilacher, 2007). De Lestang (1965) summarized results acquired by teams of petroleum geologists (SNPA, BRP and PetroPar). This initial set of publications is the basis for subsequent geological and hydrogeological synoptic works (Deynoux et al., 1985; MEH, 2015; Schneider and Wolff, 1992; Trompette, 1983; Fig. 2). Sedimentary logs representative of the Ennedi stratigraphy in Sudan were provided by Klitzsch et al. (1993). On a larger scale, and as the Palaeozoic of the Ennedi Plateau belongs to the Erdi Basin, which is itself the Chadian southern counterpart of the Kufrah basin (Bellini and Massa, 1980; Bellini et al., 1991; Turner, 1980), comparisons can be made with the adjacent Libyan outcrops and subsurface data, where renewed petroleum exploration has taken place during the last two decades. Le Hérissé et al. (2013) and Page et al. (2013) described latest Ordovician-earliest Silurian palynomorphs and graptolites, respectively. The latter provide some constraints on the age of the fine-grained deposits responsible for the softer "Intra-Tassilian Trough" identified close to the Chad-Libya boundary, which, however, appear older than the classical lower Silurian graptolitic shales. Last, it has been shown that the lower Palaeozoic succession was truncated by a system of late Palaeozoic (early Carboniferous?) ice-stream troughs (Le Heron, 2018; Le Heron et al., 2022).

This paper presents preliminary results on the Lower Sandstones exposed near the town of Fada (Figs 1 and 3), the erosion of which contribute to the magnificent landscapes of the *Ennedi Natural and Cultural Reserve* (https://www.africanparks.org/the-parks/ennedi). Relationships with the underlying basement, depositional facies and a refined stratigraphic scheme, as well as the end-Ordovician glacial/post-glacial record will be successively described, completing earlier studies. Finally, the significance of this Ordovician proximal sedimentary record in the overall stratigraphic framework of the Gondwanan cratonic platform is highlighted.

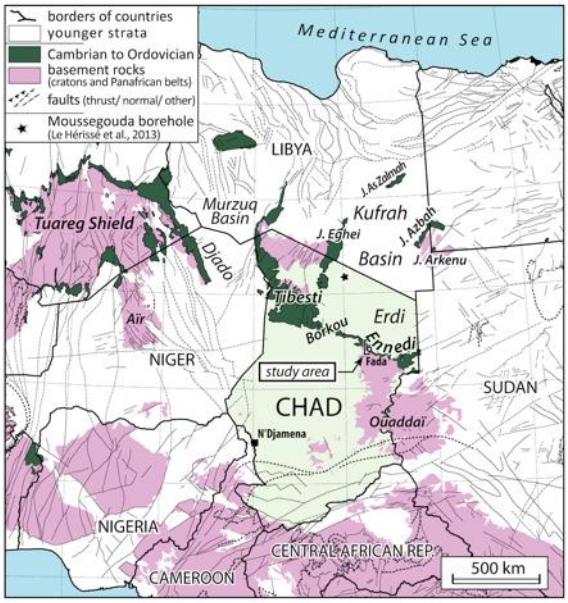

Fig. 1. *Location map. South of the Kufrah Basin The Ennedi plateau (NE Chad) exposes the southern margin of the Erdi Basin (modified from BRGM, 2004; De Lestang, 1965; Le Heron et al., 2015).*

2. Lithostratigraphy of the Lower Sandstones and former age attributions

Initially understood as Silurian strata due to the early discovery of *Harlania* ichnofacies (Lacroix and Tilho, 1919; at a time when the Ordovician System was yet not established as such), the Lower Sandstones of the Ennedi were later considered as Ordovician (Wacrenier, 1958). Afterwards, De Lestang (1965) briefly describing the succession distinguished from the base to the top: (i) the formation of the 'Basal Sandstone of the Ennedi', which he assigned to the Cambrian; (ii) a Silurian Wadi Djoua Fm. characterized by ferruginous sandstones; (iii) a fine-grained interval (shales and sandstones, subordinate limestones), referred in northern Chad to as the Bedo Fm., and (iv) the Silurian-Lower Devonian sandstones constituting the Gouring Fm.; the four subdivisions defining together the Borkou Group, the two former corresponding more specifically to the Lower Sandstones (Fig. 2). The Lower Sandstones, however, have since been generally assigned to a Cambrian-Ordovician time interval (Trompette, 1983).

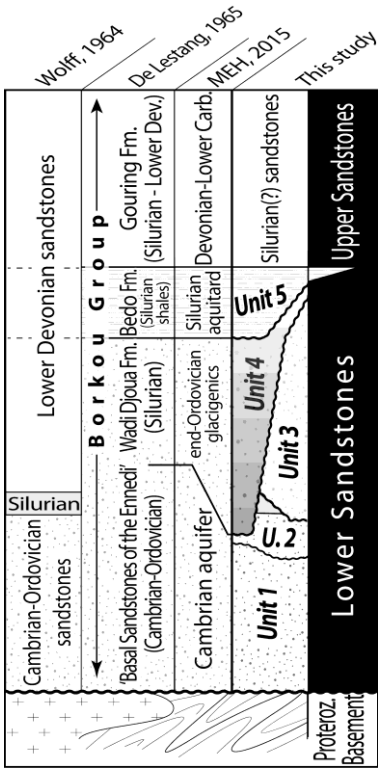

Fig. 2. *Lithostratigraphic framework and age attributions for the Lower Sandstones of the Ennedi. Four allostratigraphic units (units 1-4) have been identified in the present work. The Bedo Fm. (Unit 5), which separates the Lower from the Upper Sandstones, behaves morphologically like the Lower Silurian shaly units across the Sahara, although it may mainly correspond to an uppermost Ordovician interval. Note that another shaly interval positioned at a lower level within the Lower Sandstones (upper part of Unit 2) has been considered Silurian in some previous works.*

As noted by Schneider and Wolff (1992), the previous assignment to the Silurian of a shaly horizon responsible for a cuesta mimicking the intra-Tassilian Trough, but positioned well below the Bedo Fm., leads to a pertaining confusion in geological maps where a significant part of the Lower Sandstones is thus wrongly included in the Silurian-Devonian Upper Sandstones (e.g., Wolff, 1964; Fig. 2). The most recent hydrological mapping project (MEH, 2015) recognizes the true position of the Bedo Fm. in the Ennedi (see also Klitzsch, 1965b; De Lestang; 1965) and in addition identifies right below an underlying conglomeratic unit that they attributed to an end-Ordovician 'tillite'. They however consider the Lower Sandstones below the latter as a Cambrian rock unit, which suggests preglacial Ordovician

strata would be lacking in the Ennedi (Fig. 2). However, an essentially Ordovician age will be argued in what follows for the Lower Sandstones of the Ennedi.

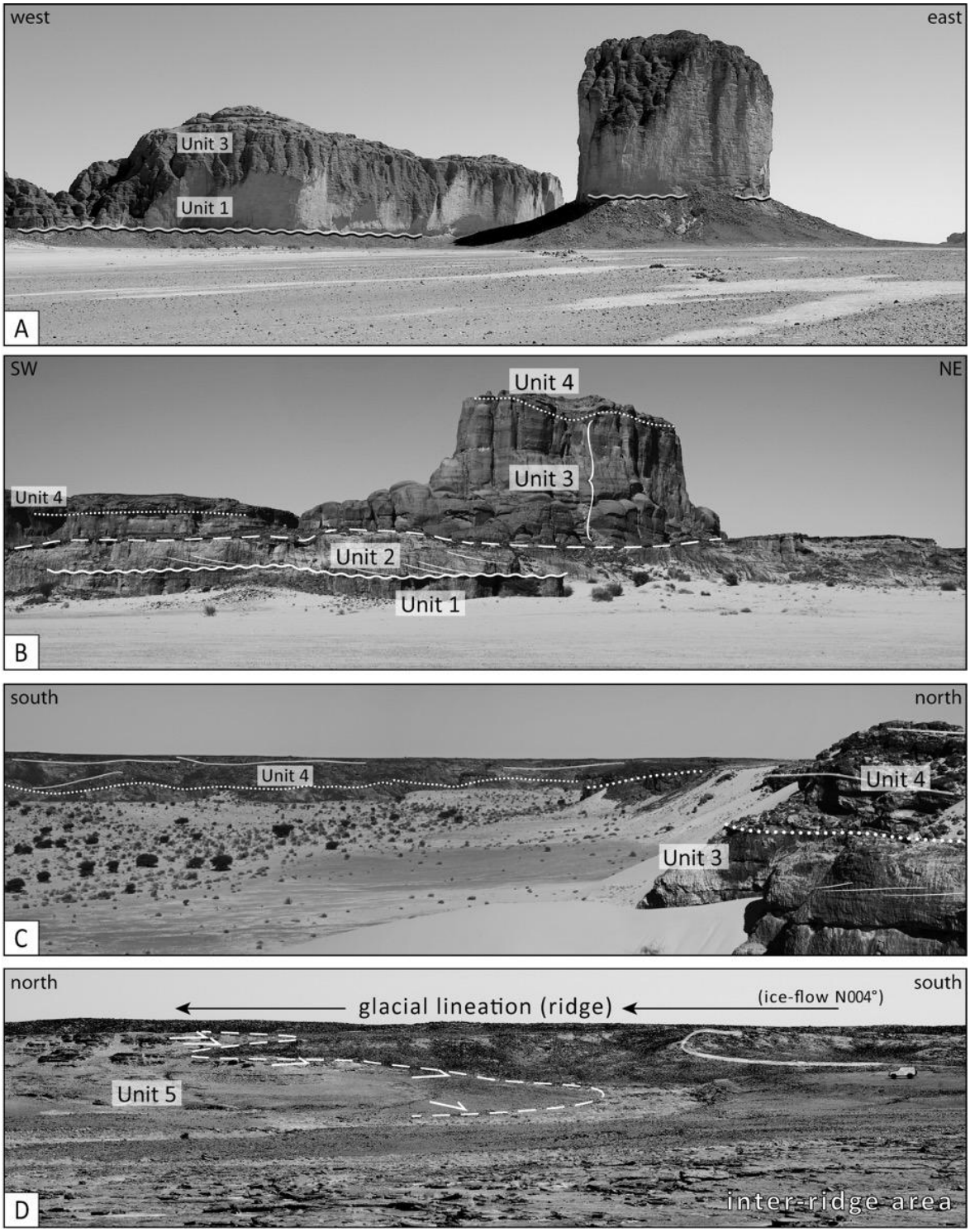

Fig. 3. *Panoramas showing the characteristics of the Lower Sandstones, from south to north of the study area.* ***(A)*** *The essentially flat lower contact over Proterozoic basement rocks (Deli-Borototou mountain, c. 300 m high). In this particular area, Unit 1 and Unit 3 amalgamate and, further, amalgamation with the Upper Sandstones is suspected (see Fig. 4).* ***(B)*** *Erosional lower bounding contacts of Unit 2 on Unit 1 (wavy line), and of Unit 4 on Unit 3 (dotted line). The fine-grained interval at the top of Unit 2 (not seen) controls the development of a cuesta and mesa. Large-scale cross-strata in Unit 2 are highlighted (Bogaro area; Unit 3 thickness: c. 80 m; see also Fig. 5C).* ***(C)*** *The regional-scale erosional and undulating contact (dotted line) at the base of the glaciation-related Unit 4 (wadi Djoua Fm.), which itself includes several, second-order, internal erosional surfaces (see Fig. 4).* ***(D)*** *The onlap relationships (white half-arrows) between the fine-grained deposits characterizing Unit 5 (Bedo Fm.) and a late glacial erosion surface, which is partially exhumed and displaying relics of > 20 m-high glacial lineations (see also Fig. 7D). The latter are locally reworked*

by iceberg furrows (highlighted cirque behind the 4x4; shown with a star in Fig. 7D; Wadi Torbo, Bideyat area).

3. The Lower Sandstones in the Fada area: overview and basal bounding surface

3.1. *Study area and large-scale architecture*

The Lower Sandstones have been investigated from the Deli-Borototou mountain (basal contact) to the Wadi Torbo area (upper contact), 40 km to the south and 35 km to the WNW of the town of Fada, respectively. The corresponding submeridian outcrop band dips slightly to the NE and consequently exposes progressively younger strata from south to north. Sandstones emerge from the sand cover in the form of either poorly accessible escarpments, mesa and pinnacles or, alternatively, as extensive horizontal exhumation surfaces (Fig. 3). In the Fada area, the total thickness of the Lower Sandstones is *c.* 200 m. Here we successively describe four allostratigraphic units (Units 1-4) bounded by erosion surfaces from the base to the top of the Lower Sandstones (Fig. 4). In addition, an overlying Unit 5 is described, which essentially corresponds to the shaly Bedo Fm. of De Lestang (1965). Indeed, the Bedo Fm. is still potentially uppermost Ordovician in age, provided the correlation with the fine-grained interval studied by Le Hérissé et al. (2013) and Page et al. (2013) is valid.

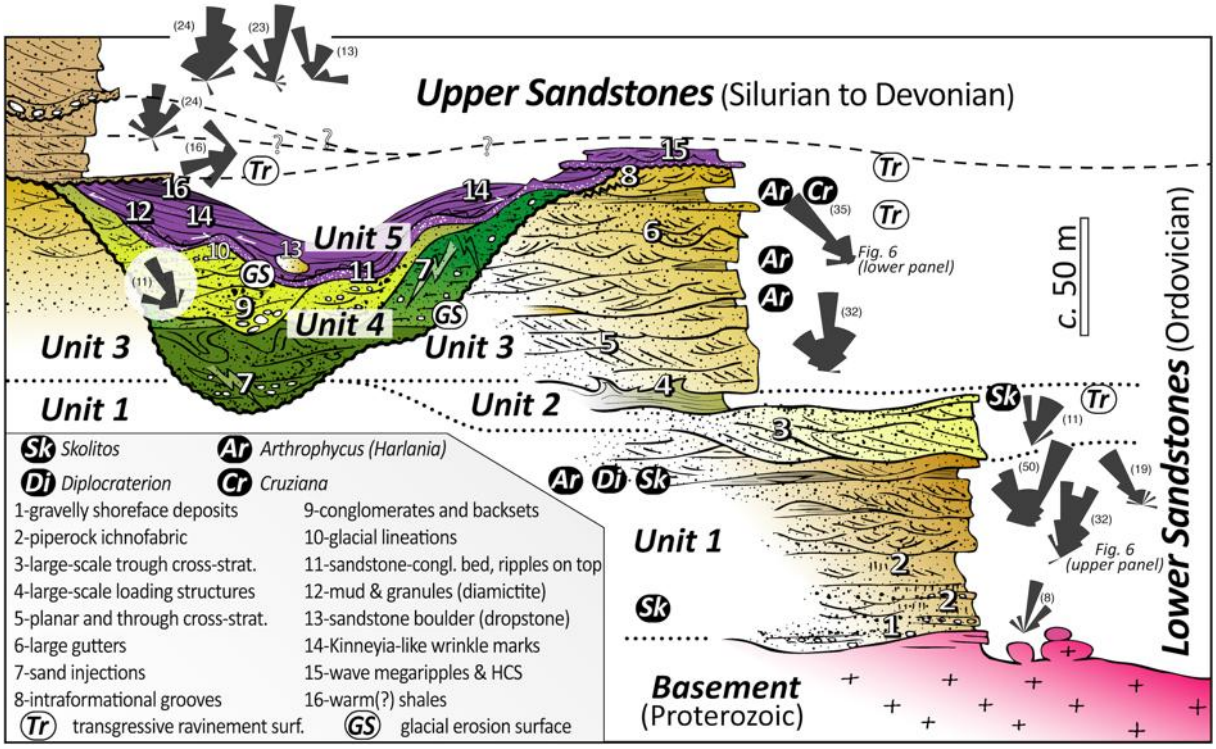

Fig. 4. Overview of the Lower Sandstones stratigraphy*, which, above the lower unconformity including a lateritic profile, is subdivided in four erosion-based units (see also Figs 2 and 3). Unit 4 includes several erosion-based units and is waiting for a more detailed framework. Note repeated amalgamations where intervening units could not be identified due to non-deposition (interfluve areas) or their subsequent erosion (cf. Fig. 3A). Unit 5 (purple, Bedo Fm.) does not belong to the Lower Sandstones, but may be essentially very latest Ordovician in age, with Lower Silurian strata possibly preserved only toward the top of the unit ('warm' shales, Fig. 5F). Geographic coordinates in Table 1.*

Note that the deep, glaciation-related, erosion surface marking the base of Unit 4 may locally cut down into Unit 2, in which case Unit 3 is absent. Also, Unit 2 is absent (or at least non-individualized) in places, in which cases Unit 3 amalgamates with Unit 1 along a poorly identifiable contact. As well, Unit 4 and Unit 5 are locally very thin or absent, in which case Silurian sandstones of the Gouring Fm. rest almost directly onto, or locally amalgamate with Unit 3 (Fig. 4). This architecture probably explains the various stratigraphic assignments proposed in the literature (Fig. 2). Additional work is needed to specify at the regional scale the maximum erosion depths for each of the erosional boundaries.

3.2. *The basement-cover unconformity*

The Lower Sandstones rest in sharp contact with the underlying Panafrican basement comprising granites, gneiss or quartzite ridges (Saharan metacraton of Liégeois et al., 2013). The geometry of the contact in the Deli area is essentially horizontal at the km-scale (Fig. 3A), but in places displays an undulating surface comprising up to 5 m-deep depressions. In this case, the sandstone cover shows gentle onlapping relationships. Where consisting of granites, the uppermost basement rocks show a well-defined tripartite succession, from base to top: massive, weathered granites, outcropping as m-scale balls; deeply weathered granites, corresponding to a soft, up to 5 m-thick, whitish, clayey horizon; a 'stratified' unit, 3-8 m in thickness made up of weathered and more or less rubified granites. At the basement-cover contact, a pebbly lag shows dispersed quartzite cobbles up to 15 cm in diameter.

Interpretation. A thick weathering profile thus developed before the onset of sand accumulation, and it has been largely preserved. Part of the rubefaction is however suspected to correspond to a later diagenetic imprint. Nevertheless, the nature of the pebbles underlining the basement-cover contact — only quartzite, no granite or gneiss — also substantiates a former, intense, weathering phase that left behind only clasts representative of the more resistant lithologies. Depressions might indicate an intervening erosion phase developing a paleo-drainage network after weathering but prior to deposition of the quartz-rich sediment cover. The weathering profile is reminiscent of the lateritic profile described by Germann et al. (1993) in NW Sudan.

4. The Lower Sandstones: preglacial units 1-3

4.1. *Unit 1 (lower part of the Lower Sandstones, Figs 3, 5 and 6)*

The cliff-forming Unit 1 is up to 80 m thick. It shows a sandstone-dominated, mainly coarse-grained and cross-stratified succession. At the very base of Unit 1, a specific 3-6 m-thick subunit is individualized. The latter is characterized by alternating gravel conglomerates — which are relatively well sorted (n°1 in Fig. 4) —, and coarse-grained sandstones either intensively bioturbated (*Skolithos* piperock ichnofabric) or made up of 5-20 cm-high, distinctively fining-up, cross-stratified sets showing low-angle laminae. Some of these horizons are radioactive (high U and Th contents; Schneider and Wolff, 1992). Above, coarse to very coarse sandstones with prevailing cross-stratification are dominant. Active burrowing is still noted, with some recurrences of piperock ichnofabric. *Cruziana* tracks, reported from the base of the succession by Wacrenier (1958) have not been found.

In the middle part of Unit 1, larger-scale and coarser-grained trough cross-strata show less burrowing, with dispersed, rare, or absent(?) *Diplocraterion*. The troughs are consistently oriented toward the NNE (rose diagrams, Fig. 4; satellite imagery, Fig. 6).

In the upper part of Unit 1 (Fig. 4), sandstones show a cyclic pattern corresponding to the superimposition of 3-6 m-thick, erosion-based, fining-up packages. Large (1-2 m high) trough cross-bedded sets of very coarse to granular sandstones, including quartz gravels and showing in place compound cross-stratification and overturned laminae, evolve upwards in progressively thinner and finer cross-bedded coarse-grained sandstones. The latter show frequent to intense, vertical to oblique burrowing. *Skolithos* may form dense networks and *Diplocraterion* is frequent. Cross-stratified sandstones are truncated by a gravel lag or a distinctive, cm- to dm-thick, fining-up granular sandstone bed. Above, but only if preserved beneath the overlying erosion surface marking the base of the next package, is a finer-grained interval. Such intervals, at the origin of discontinuous morphological re-entrants that extend at the 100 m scale, correspond either to a single, 5-30 cm-thick horizon of silty very fine-grained sandstone or to a m-thick succession of siltstones and fine- to coarse-grained sandstones (Fig. 5A). The latter can be thin-bedded (< 5 cm), cross-stratified or entirely rippled, with in places a distinctive lenticular bedding and undulating erosional contacts. Fine-grained, mm-thick laminae may underline some of the oblique laminae and reactivation surfaces are frequently observed. Such intervals show *Harlania* (=*Arthrophycus*) everywhere a favorable heterolitic sedimentation has developed.

Interpretation. Unit 1 is dominated by coastal deposits, at the transition from fluvial to nearshore environments. Basal conglomerates and related sandstones are more specifically understood as gravelly shoreface deposits (Dashtgard et al., 2009; Hart and Plint, 1995) in an overall transgressive setting; the latter being also indicated by active burrowing and the concentration of radioactive minerals (Dabard et al., 2015).

In the middle part of Unit 1, the fluvial signature prevails but then decreases again upwards in parallel with occurrences of thin but apparent shallow-marine incursions showing a tidal signature (gravel lag indicating ravinement processes, drapes of fine-grained sediments, lenticular bedding, intense bioturbation). Rippled sandstones in these finer-grained intervals are tentatively interpreted as estuarine mouth-bar deposits.

From base to top of Unit 1, a continuously aggrading framework is suggested, nevertheless recording a long-term transgressive/regressive/transgressive evolution. Because described as erosion-based fining upward packages, high-frequency ‘transgressive’ cycles are suggested as building blocks of the upper part of Unit 1. However, the cyclic pattern might alternatively represent the superimposition of ‘highstand’ regressive (large cross-bedded sets) then transgressive (bioturbated cross-bedded sandstones and overlying tide-influenced intervals) deposits. In the latter case, the erosion surface at the base of any individual package would correspond to channel bases rather than to a regional-wide subaerial erosion surface. This may explain the lack of indication for weathering in between individual cycles. An overall marginal-marine depositional environment, comprising fluvial, bay-head delta and estuarine deposits, is inferred on the basis of both primary sedimentary structures and associated bioturbation (Buatois and Mángano, 2011). Whether the high-frequency alternation of fluvial-dominated and nearshore deposits represent autogenic or allocyclic processes —

e.g. controlled by eustacy or a varying rate of sediment supply — remains to be elucidated (Zecchin, 2007).

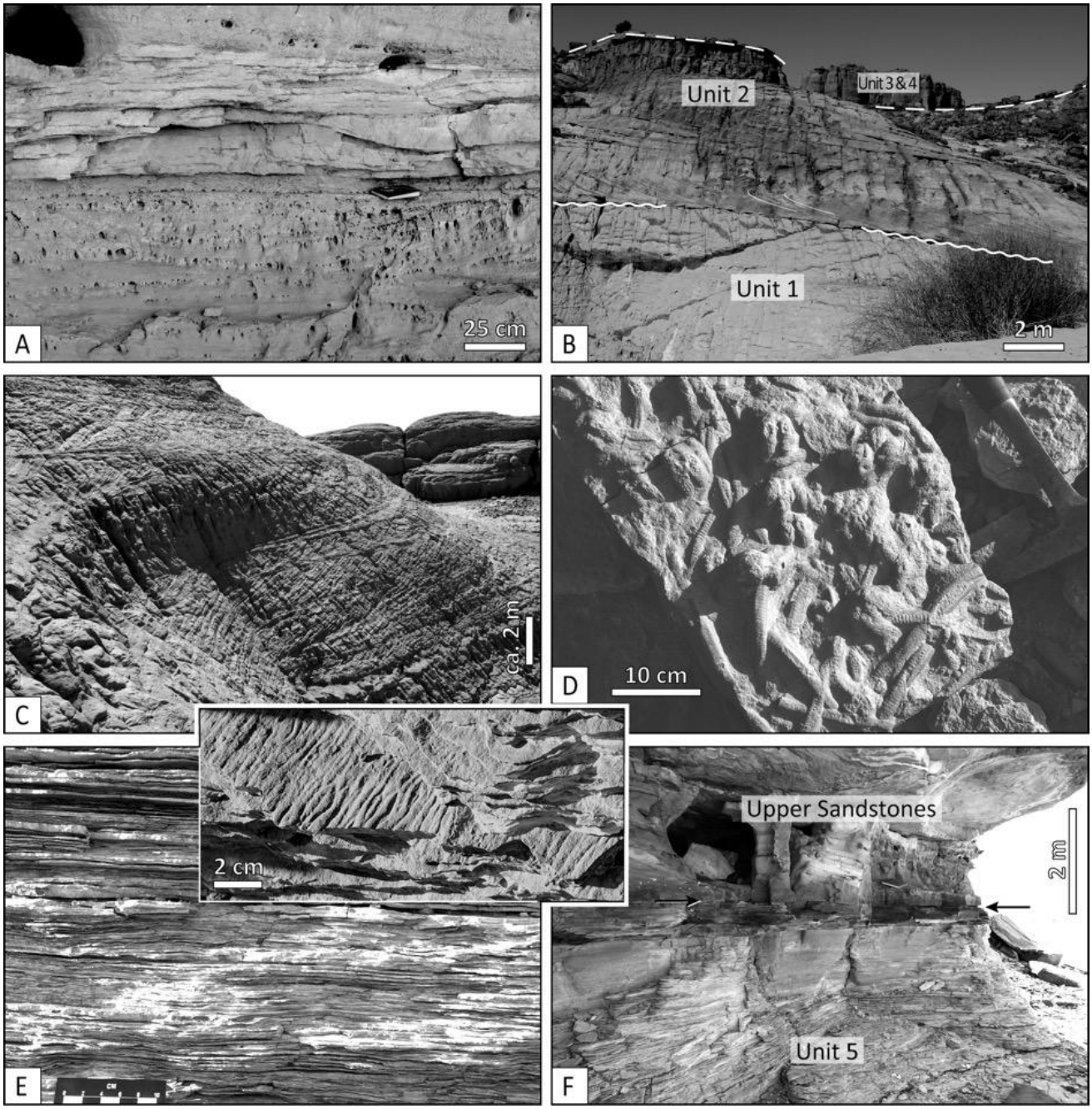

Fig. 5. *Depositional facies in the Lower Sandstones and Bedo Fm.* ***(A)*** *A tide-influenced interval (undulated bedding, heterolitics, Arthrophycus) sandwiched in between cross-stratified deposits showing a top-truncated coarse-grained, bioturbated sandstone (lower part) and an overlying erosion-based very coarse-grained, non-bioturbated sandstone (upper part of Unit 1).* ***(B)*** *Detailed view of Fig. 3B, showing the erosion-based Unit 2, large-scale and rhythmic cross-stratification (including overturned laminae; Fig. 4/3) and the truncation by a transgressive ravinement surface in its upper part (dashed line).* ***(C)*** *Mixed planar and trough cross-stratification (non-bioturbated) in the lower part of Unit 3 (Fig. 4/5).* ***(D)*** *Associated Arthrophycus and Cruziana (mainly Rusophycus forms), characterizing a singular fine-grained interbed in the upper part of Unit 3.* ***(E)*** *Rhythmically*

laminated fine-grained sandstones in the lower part of Unit 5 (Fig. 4/14). Layer tops typically show Kinneyia-like wrinkle marks (onset). ***(F)*** *The topmost part of Unit 5 made up of shales, lacking sandstone horizons (warm? shales of Meinhold et al., 2016; Fig. 4/16), and truncated by a distinctive coarse-grained sandstone bed (black arrow). Above is the base of Upper Sandstones (Silurian to Devonian). Geographic coordinates in Table 1.*

4.2. *Unit 2 (middle part of the Lower Sandstones, Figs 3B and 5B)*

Unit 2 is a relatively thin, bipartite succession resting onto an erosion surface truncating Unit 1. The main part of Unit 2 is an up to 15 m-thick, fining- and thinning-upward sequence of cross-bedded sandstones. At the base, sandstones are organized in large-scale trough cross-stratified sets, up to 4 m in thickness (Fig. 4/3). A rhythmic pattern might be identified when < 5 cm-thick granular laminae repeatedly alternate with up to 40 cm-thick medium- to coarse-grained sandstones including dispersed gravels. Upward, cross-bedded sandstones typically show thinner, m-thick sets. Bioturbation has not been observed. Cross-bedded sandstones are sharply truncated by an essentially flat erosion surface underlined by a gravel lag including some quartz pebbles at the base of a 10-20 cm thick distinctive graded sandstone bed, including poorly defined burrows (*Skolithos*?). The uppermost part of Unit 2 is a m-thick, highly ferruginized siltstone, from which primary structures have been erased. Siltstones are deformed by decameter-scale load casts affecting the immediately overlying sandstones of Unit 3.

Interpretation. A fluvial origin might be proposed from the lower cross-bedded sandstones, even if the rhythmic organization might suggest a tidal cyclicity; the advance of coarse-grained, bar-top megaripple trains would, however, also produce such a rhythmic pattern without any tidal signal. Their truncation and the related coarse-grained bed is interpreted as a marine ravinement surface overlain by a horizon of 'basal transgressive sand'. The overlying siltstones may reflect either offshore deposition or fine-grained sedimentation in the middle, low-energy segment of an estuarine system. However, diagenetic ferruginization precludes a more advanced interpretation.

Depositional environments of Unit 2 do not actually depart from the ones identified in the upper part of Unit 1 (and overlying Unit 3). A deeper basal erosion surface, larger cross-bedded sets and a (residual) 1 m-thick siltstone interval each appear as exaggerated versions of all the features characterizing cyclical packages described in the upper part of Unit 1. A larger-scale pulsation (higher amplitude? higher rates of variation?) of the factors controlling coastal sedimentary dynamics in the Ennedi is thus inferred at this level.

4.3. *Unit 3 (upper part of the Lower Sandstones, Figs 3B, 5 and 6)*

Like Unit 1, Unit 3 is a cliff-forming, up to 100 m-thick succession of essentially cross-bedded sandstones. Where Unit 2 ends with siltstones, the basal erosional contact of Unit 3 is underlined by a distinctive blue-grey, coarse-grained gravelly sandstone showing large-scale load structures (Fig. 4/4). Unit 3 is characterized by coarse- to very coarse-grained cross-stratified sandstone beds with dispersed gravels. Mixed large trough and planar cross-stratification are identified (Fig. 5C; Fig. 4/5). Neither bioturbation nor fine-grained intervals have been observed in the lower 30 m of Unit 3 but fine-grained intervals including *Arthrophycus* reappear upwards (only observed in scree deposits).

The upper part of Unit 3 is only exposed in a few preserved interfluve areas beneath the deep erosion surface characterizing the base of the overlying, erosion-based Unit 4 (Fig. 4). Medium- to coarse-grained cross-strata are observed, corresponding to 10s m wide troughs; the larger being distinguishable from satellite images and evidencing a NW-oriented dispersal pattern (Fig. 6). As in Unit 1, cross-bedded sets are organized in fining- and thinning-up packages. In contrast of the ones of Unit 1, some of the intervening bounding erosion surfaces are deeply (> 2 m) incised with pebbly lags and steep margins suggesting large-scale gutters. In addition, cross-bedded sandstones show less bioturbation than those if Unit 1. A dm-thick, distinctively well-sorted, coarse-grained sandstone bed underline in places the boundary between cross-bedded sandstones and the overlying fine-grained interval. In the latter, bioturbation includes small Cruzianids, generally *Rusophycus* forms, rarer *Cruziana* forms, which are associated, or not, with *Arthrophycus* showing well-defined annulations (Fig. 5D).

Interpretation. A large-scale transgressive trend is recorded from the base to the top of Unit 3, as evidenced by the greater development of fluvial deposits in the lower part of the unit (including, frequent planar cross-stratification), the overall fining-up trend and ichnofacies changes (no bioturbation, then *Arthrophycus*, then *Arthrophycus* and *Cruziana*). Though it remains to be confirmed, a lesser development of the *Skolithos* ichnofacies seems to be noted in the whole of Unit 3 when compared to Unit 1. Well-sorted sandstone beds separating fluvial sandstones from marine, bioturbated intervals are interpreted as the signature of marine ravinement processes, possibly by tidal currents.

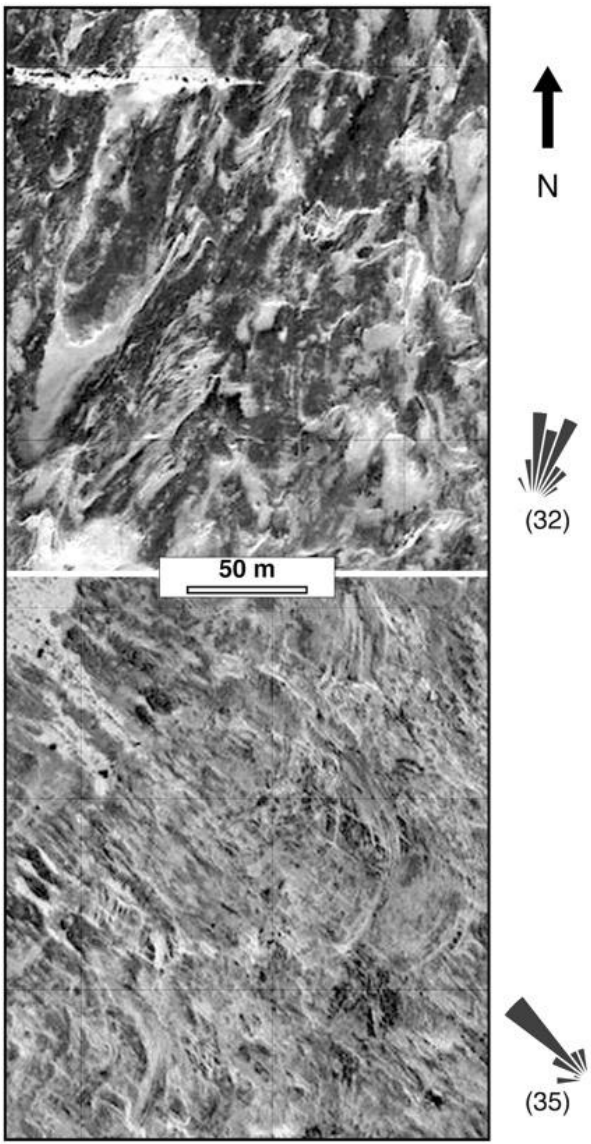

Fig. 6. *Satellite images illustrating two types of large-scale trough cross-stratification in the Unit 1 (upper panel) and Unit 3 (lower panel) of the Lower Sandstones. Rose diagrams of cross-stratal dips were made from areas near (< 3 km) the views (stratigraphic locations in Fig.4; geographic coordinates in Table 1).*

5. The record of the end-Ordovician glaciation: units 4-5

5.1. *Unit 4 (uppermost part of the Lower Sandstones, Wadi Djoua Fm., Figs 3D and 7)*

Unit 4 constitutes the infill of several tens of meters deep incisions truncating Unit 3, which are themselves truncated by the erosion surface marking the base of Unit 5 (Fig. 4). Unit 4 consists of a variety of massively bedded to cross-stratified sandstones, with various abundance of dispersed pebbles. Sandstones locally grade into conglomerates with dispersed quartzite cobbles up to 20 cm in diameter. Unit 4 is furthermore characterized by discontinuous chaotic outcrops that include cuesta-like slopes at the km-scale, large-scale (> 100 m) sigmoidal and channelized sandstones bodies, sand injections in the form of 5-15 cm-thick ferrugineous dikes or sills (Fig. 4/7), and three-dimensional folding structures affecting 1-3 m thick sandstone horizons.

No paleovalley network has been properly identified so far, yet WNW-EWE-oriented depressions have been inferred, in agreement with paleocurrent trends (Fig. 4). In‘interfluves’ area, Unit 4 is essentially missing and a thin or absent Unit 5 rests directly on Unit 3. Unit 4 is equivalent to the Wadi Djoua Fm. of De Lestang (1965) (Fig. 2). However, this author reported dolerite intrusions in this formation, which we did not observe.

A detailed facies succession in Unit 4 remains to be established and only preliminary observations are provided below. The basal bounding surface and immediately overlying sandstones were generally affected by heavy ferruginization, which hinders the identification of probable onlaps relationships. Conglomeratic facies associations appear preferentially in the lower part of the unit, while the initial deposits that directly seal the basal erosion surface of Unit 4 are, in places, made up of relatively well-sorted coarse-grained sandstones. Cut-and-fill structures 0.5-5 m-deep and 5-50 m in width show alternation of well- to faintly-laminated coarse-grained sandstones and clast- or matrix-supported pebbly conglomerates with dispersed cobbles. Undulating laminae, backsets and pebbly lags are noted (Fig. 7E). Clasts are subangular to subrounded. Clast lithologies are both extrabasinal (vein quartz, fine-grained, granular or gravelly quartzites, rare cherts) and intrabasinal (sandstones and siltstones). The latter may constitute intraformational conglomerates, with siltstones intraclasts up to 60 cm-long and a poor representation of extra-basinal clasts. Such conglomeratic deposits progressively grade upward in coarse- to medium-grained, trough cross-stratified sandstones. Together they constitute tens of m-thick, fining- and thinning-upward sandstone sequences. Such successions include in places m-thick intervals of thinly bedded, fine- to medium-grained sandstones with rippled tops and small-scale load casts, and are locally truncated by sandstone beds characterized by abundant rip-up clasts at their top. Though the former have a limited extent (10s to 100s of meters), the latter constitute extensive, horizontally stratified marker beds at the km- to 10s km-scale, which sharply

truncate the underlying chaotic and locally deformed sandstones forming the main infill of the incisions.

Interpretation. The deep basal erosion surface, the overall chaotic organization, the conglomerates with numerous extra-basinal clasts, and the stratigraphic position immediately beneath a well-identified glacial surface (see Unit 5) allow Unit 4 to be interpreted as a glaciation-related depositional unit. Similar facies associations including subglacial sedimentary injections and large-scale channels have been documented in the Felar-Felar Fm. of the Djado Basin (north Niger; Denis et al., 2010) and in the Mamuniyat Fm. of the Kufrah Basin (southeastern Libya; Le Heron et al., 2010, 2015). Large intrabasinal clasts and bedding/lamination patterns that indicate supercritical flow processes noticeably depart from the other fluvial deposits described in units 1-3 and also support the glacigenic interpretation (Girard et al., 2015; Lang et al., 2021). No striated pebbles have been, however, identified so far. This is usually the case in bedload dominated deposits, where tractive processes rapidly erase potential glacial striae. Cryptic intraformational glacial erosion surfaces might be suspected owing to the occurrence of large-scale folds and massive sandstones, which could represent deformation tills especially where they are intruded by networks of sandstone dikes (Ravier and Buoncristiani, 2018). Channelized and sigmoidal sandstone bodies at the 100s m scale in one hand, and intervening finer-grained intervals including flaser bedding and load casts are reminiscent of end-Ordovician meander belts (Rubino et al., 2003). Fluvio-glacial dynamics in an ice-marginal context is therefore predominant in Unit 4, though intervening subglacial deformation events are also suspected. Sandstone marker beds are tentatively interpreted as subordinate transgressive horizons, a better identification of which should help to establish a more detailed stratigraphic succession in Unit 4.

5.2. *Unit 5 (Bedo Formation, Figs 5 and 7)*

Unit 5 was observed close to Wadi Torbo, where it is discontinuously but frequently exposed over a *c.*100 km^2 area. Elsewhere, Unit 5 might not be individualized (for instance, south of Fada; Fig. 3A), in which case the identification of the contact between the amalgamated Lower and Upper Sandstones is challenging (Fig. 4). Unit 5 is mainly comprised of a fine-grained succession including an intervening sandstone interval. This succession onlaps at the outcrop scale a corrugated surface shaping the ferruginized top of an underlying sandstone (white arrows in Fig. 7D).

The corrugated surface is shaped in parallel, north-south (N 04±1°) oriented ridges and troughs (Fig. 7B). Wavelengths and amplitudes are in the 250-500 m and 5-30 m ranges, respectively. Some of the corrugations can be followed individually on distances > 3 km (Fig. 7A). Rectilinear, smaller-scale (<10 m wide), second-order and parallel sandstone ridges show higher elongation ratios (Fig. 7D). Beneath the corrugated surface, the fine-grained succession is almost everywhere underlined by a continuous, < 1m-thick, sandstone/conglomerate bed, which therefore appears to be also conformable to an underlying, undulating erosion surface (Fig. 4/11). Small-scale extensional step fractures are ubiquitous in the coarse-grained bed. Only one isolated (displaced) stone bearing striae was discovered. In a single outcrop, N-S-oriented poorly defined intraformational grooves have been observed in the underlying Unit 3 one meter below the Unit 5/Unit 3 contact (Fig. 4/8).

The sandstone/conglomerate bed locally shows a pebbly lag at its upper surface and is systematically capped by trains of current ripples atop a cm-thick veneer. The lag and the ripple trains mold m- to several m-scale gullies or depressions that add local complexity to the otherwise relatively smooth corrugated surface. Satellite images reveal that the corrugation field is disrupted by 25-60 m wide furrows with lateral and frontal berms. Their orientation ranges from N350 to N30, the frontal berm being positioned to the north (Fig. 7C).

The fine-grained succession above the corrugation field starts with a thin (5-20 cm) muddy sandstone or siltstone horizon including in places isolated quartz granules. Above, and constituting the main part of Unit 5, are laminated, whitish, clayed siltstones including various proportions of fine-grained, thin-bedded sandstone (mm-scale 'laminae' to cm-scale beds). Rhythmical patterns are frequently observed at the 10-20 cm scale. A sandstone boulder has been found isolated in the lower part of Unit 5 (Fig. 4/13). A more indurated horizon is in addition usually observed within the soft, fine-grained succession. Its nature and position are variable from place to place, yet usually observed in the lower part of Unit 5 (Fig. 4/14). Additional work is needed to confirm it represents a correlatable horizon. In troughs, this horizon may not fundamentally differ from the laminated siltstones (less clayed?) or corresponds to a few m-thick, heretolitic interval characterized by a flaser to lenticular bedding at the mm- to cm-scale. In this case, Kinneyia-like wrinkle marks repeatedly characterize bed tops, showing a consistent N20-N200 orientation (Fig. 5E. Fig. 4/14). Laterally, where Unit 5 thins out over 'paleohighs' (the highest ridges of the corrugation field, i.e., less eroded interfluve areas), a single coarse-grained sandstone bed, 20-40 cm-thick, relatively but distinctively well-sorted, shows cross-stratification and, in some places, megaripples with preserved primary relief (Fig. 4/15). An intraformational conglomerate of rip-up siltstone clasts occasionally underlines the lower bed contact. Above, dm-thick, fine-to medium-grained sandstone beds show in places HCS laminations with parting lineations and/or *Arthrophycus*.

The uppermost 2 m of Unit 5 consists of shales (Figs 5F and 4/16). This is the finest-grained interval of Unit 5, enhancing an overall fining-upward pattern. Unit 5 is sharply truncated by a dm-thick gravelly sandstone bed underlining the trough cross-bedded Silurian-Devonian Upper Sandstones. The latter consist of medium- to coarse-grained sandstones including recurrences of siltstone horizons and bioturbations, mainly tracks along horizontal truncation surfaces. Palaeocurrent trends noticeably deviate to the west or SW (Fig. 4). Upper Sandstones grade upwards into coarse- to very coarse-grained deposits, with resumption of palaeocurrent trends toward the north.

Note that due to onlaps onto the corrugation field (Figs 4 and 7), Unit 5 is most often incomplete; Unit 5 being reduced to a few m-thick interval above some of the highest ridges. The lowermost Upper Sandstones have a wider distribution but might also be absent (or undifferentiated?). It has not been established whether their absence is related to non-deposition or to truncation beneath one of the erosion surfaces locally underlined by intrabasinal conglomerates within the lower part of the Upper Sandstones (question marks in Fig. 4).

Interpretation. The corrugation field is interpreted as an exhumed a glacial surface. The ridge-and-trough organization and superimposed second-order ridges correspond to streamlined

glacial lineations developed over a soft sediment substrate (Deschamps et al., 2013; Le Heron et al., 2022; Moreau et al., 2005). In this context, the sandstone/conglomerate bed draping the undulating basal truncation likely corresponds to a subglacial fluidized horizon (Denis et al., 2010). In association with late step fractures and underlying intraformational shear structures such as grooves, this bed highlights a soft-sediment subglacial shear zones (Denis et al., 2010; Girard et al., 2015; Le Heron et al., 2005). In map view the Chadian corrugation field resembles assemblages of Quaternary megascale glacial lineations (MSGL), but we note however that: (i) the width of the highly-elongated second-order ridges is noticeably smaller than that of typical MSGL; and (ii) conversely, the height of the first-order corrugations, in excess of 20 m, is largely greater than that of typical MSGL (Spagnolo et al., 2014). This suggests that the corrugations fit a specific category of glacial lineations, characterized by vertical amplitude greater than 20 m, which might represent forms that are transitional with elongated drumlins (Spagnolo et al., 2014). It is in addition noted that the core of the corrugations is made up of non- to slightly deformed Unit 3 sandstones. Glacial lineations observed in Wadi Torbo are therefore interpreted as having been formed according to a drumlinization model accounting for the erodent layer hypothesis (Eyles et al., 2016). Initial drumlins essentially shaped by carving in pre-existing bed material were progressively reworked into ridges under an accelerating ice stream. Delicate features preserved at the former ice-sediment contact (striae, grooves…) were not preserved due to active and generalized post-glacial winnowing evidenced by ripple trains (tidal pumping close to a retreating grounding line?). Only the largest structures were preserved, such as gullies (formed by gravity-driven instabilities?), furrows and associated berms (ploughmarks of northward-drifting icebergs) or depressions (marks of keels of stranded icebergs?). A potential analogue of this palaeo-landsystem is the Barents Shelf (Newton and Huuse, 2017), considering the intracontinental setting, moderate water depths, MSGL size and cross-cutting relationship with iceberg ploughmarks.

Granules dispersed in siltstones and muddy sandstones draping the glacial lineations most likely record ice-rafting processes. Interestingly, no outwash facies have been identified. Overlying laminated siltstones, lacking ice-rafted clasts —with, however, the notable exception of the sandstone boulder—, lacking storm-generated facies and bioturbation, but showing rhythmical stratification pattern are tentatively interpreted as the settling of hypopycnal meltwater plumes beneath a perennial sea-ice cover (Rüther et al., 2012). In this case, and accounting for high ice-marginal accumulation rates, the time span represented by the fine-grained Unit 5 might be relatively short (Lucchi et al., 2015). The sea-ice cover hypothesis is favored relative to an ice-shelf model because of the shallow water depths, the lack of ploughmarks from large tabular icebergs, and the lack of facies marking the retreating calving-line (Smith et al., 2019). The more conservative interpretation that would simply consider a restricted-marine depositional environment for the Bedo Fm. cannot be ruled out.

In this context, the significance of the intervening coarser-grained interval observed in the lower part of the Bedo Fm. remains unclear: the break-up of the ice cover and restoration of storm processes?; temporary re-advance of a groundling line?; transgressive deposits involving a healing phase (Proust et al., 2018)? Over the adjacent highs, HCS beds and megaripples, which are the signature of combined flow deposits in fine- to medium-grained, and coarse-grained sands, respectively (Leckie, 1988), might be the proximal counterpart of

such a healing phase. In any case, wave processes suggest that the Ennedi was affected at that time by relatively open-marine conditions.

The presence of Kinneyia-like structures, most likely linked to microbial mats (Aubineau et al., 2018) suggests a tidal influence with cyclical, microbially-mediated, hydrodynamic instabilities (Thomas et al., 2013). Crest orientation of the wrinkle marks conforms to submeridian depositional slopes, i.e., dipping almost parallel to the axis of former glacially cut overdeepenings. The development of microbial mats is, however, inconclusive regarding the presence, or the termination, of a sea-ice cover. The overall Unit 5 might be the signature of an ice-front retreat during a glacio-isostatically induced forced regression rather than that of a postglacial transgression (Dietrich et al., 2019). Only the 2 m-thick shale horizon at the very top of the Bedo Fm. suggests an ultimate, post-glacial sea-level rise.

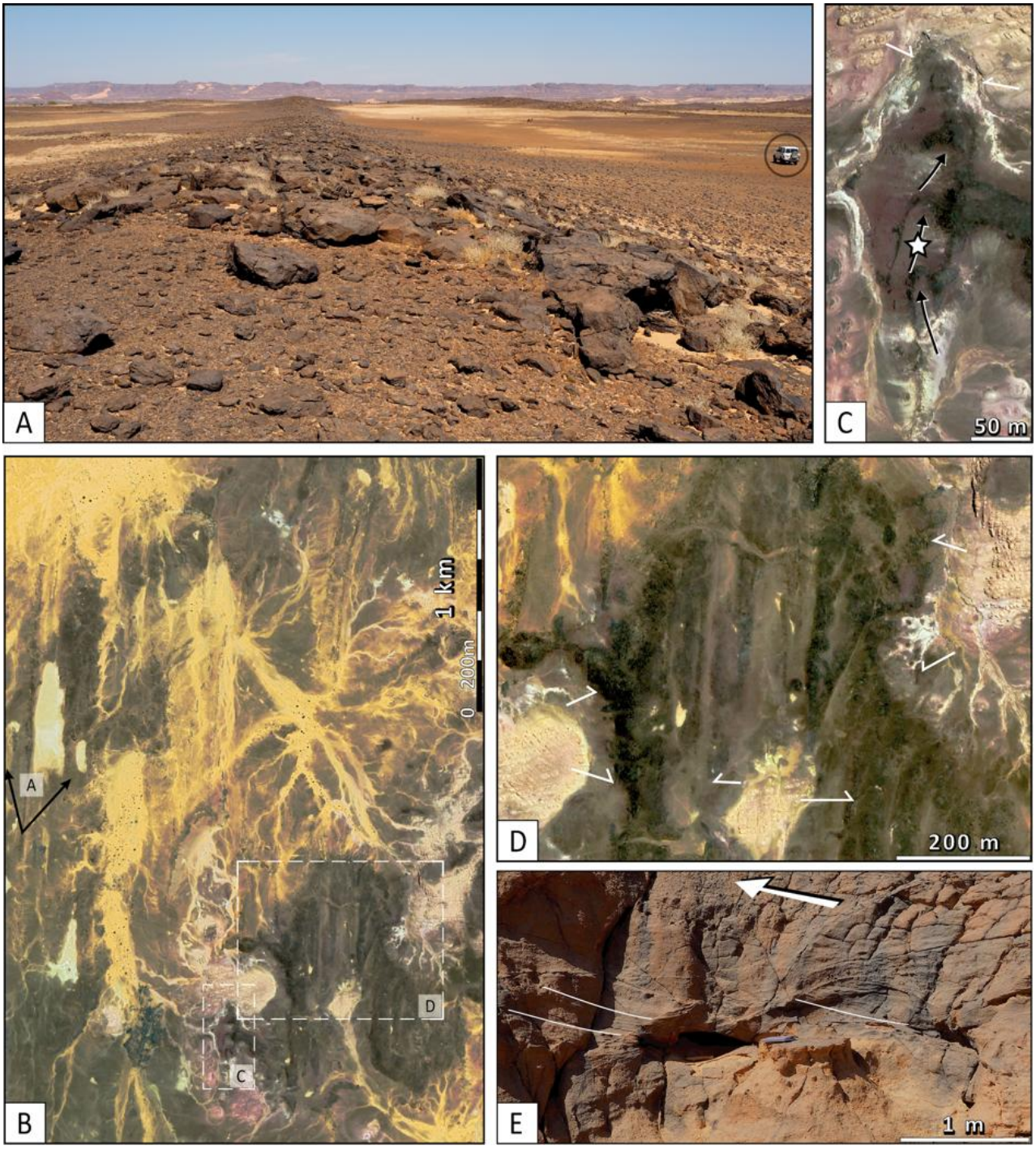

Fig. 7. *The end-Ordovician glacial record in the Ennedi.* ***(A)*** *A streamlined glacial lineation of the corrugation field at the lower part of Unit 5 (location in Fig. 7C; 4x4 for scale).* ***(B)*** *Satellite view (GoogleEarth image) of the corrugation field of the Wadi Torbo area, showing a north-oriented (N004°) ridge-and-trough topography and superimposed second-order ridges (image center at 17,33°N, 21,33°E). Close-up views of* ***(C)*** *superimposed furrows interpreted as iceberg ploughmarks reworking a glacial lineation (star: see Fig. 3D) and* ***(D)*** *second-order ridges onto a larger-scale ridge. White half-arrows highlight the onlaps of Unit 5 deposits (light colored residual patches) onto the sandstones (dark) corresponding to glacial lineations of higher elevation (Fig. 4/13).* ***(E)*** *Pebbly sandstones of Unit 4 recording prevailing upper-flow depositional processes (Fig. 4/9; faint and/or undulated laminations, backsets, intrabasinal cobbles). Highlighted backsets (white), flow almost from right to left (black arrow).*

The truncation of the Bedo Fm. by cross-bedded sandstones showing paleocurrents departing from regional trend (Fig. 4) is interpreted as an extensive marine ravinement surface overlain by tidal sandstones. An unconformity and a major hiatus are thus inferred at the top of the late- to postglacial shale-dominated sedimentation. Similar relationships are also been identified in the analogous succession of the southeastern Kufrah Basin (Turner, 1991), which interestingly differs from more continuous regressive trends interpreted from more basinal areas (Lüning et al., 2010; Gindre et al., 2012).

6. Discussion: Significance of the Ennedi record

6.1. *The preglacial succession*

The study area is located at *c.* 600 km to the SSE and SSW from the closest outcrop belts fringing the Kufrah Basin (Jebel Eghei and Arkenu area, respectively), and at *c.* 900 km to the ESE from the Djado (Niger). Considering NNE- to NW-ward oriented paleocurrents, the study area is representative of one of the innermost segments of the Gondwana shelf (Figs 1 and 4). In the absence of biostratigraphic dating, only attempts at regional correlation can be proposed for the Lower Sandstones of the Ennedi. The latter are comparable in terms of depositional environments to the Lower Sandstones around the southeastern Tuareg Shield in northern Niger (also kown as the Timesgar sandstone; Joulia, 1959) and SE Algeria (sometimes referred to as the Tin Taharadjeli Member; Beuf et al., 1971). The stratigraphic assignment of these strata has long been controversial. While a Cambrian to lowermost Ordovician age is often proposed (e.g., Eschard et al., 2010; Greigert et Pougnet, 1967; Perron et al., 2018), the same succession is regarded in the Tassili area as Ordovician by Legrand (1974, 2002), Richet and De Charpal (1995) and Fabre and Kazi-Tani (2005). The Lower Sandstones of the Ennedi are also similar to successions exposed in the Kufra Basin (fluvial sandstones with overturned cross-stratification, tidal bars, superimposed m-scale cycles, among others; see detailed description by Turner, 1980). Originally attributed to a Cambrian Hasawnah Fm. (Bellini and Massa, 1980), the upper portion of the Lower Sandstones of the Kufrah Basin is today mostly correlated with the shallow-marine, (?Lower to) Middle Ordovician Hawaz Fm. of the Murzuq Basin (Anfray and Rubino, 2000; Gil-Ortiz et al., 2022). This revision results from the generalized observation in SE Libya of bioturbated sandstones including *Skolithos*, *Arthrophycus* and *Cruziana* (Ghienne et al., 2013; Le Heron and Howard, 2012; Lüning et al., 1999; Seilacher et al., 2002). Of particular interest is a change in sedimentation identified at *c.* 200 m beneath the glacially-related strata in the Jebel As Zalmah area, involving a basal conglomerate, a significant transgressive episode and an

overall change from prevailing trough cross-strata below, to planar cross-strata above (Le Heron and Howard, 2012); all of these features being reminiscent of Unit 2 and its relationships with Unit 1 and Unit 3 of the Ennedi (Fig. 4). Unit 2 might also correlate with the middle part of the Lower Sandstones of the Jebel Arkenu (Turner, 1980) and the lower Araske Fm. of the Tibesti (De Lestang, 1965). It is worth noticing that in the Ennedi, the Lower Sandstones include bioturbated coastal deposits since their very base, lacking the thick fluvial deposits characterizing the lower/lowermost part of the Cambrian-Ordovician succession in the more distal Murzuq Basin (Elicki et al., 2019; Ghienne et al., 2013).

As a working hypothesis, and considering the occurrence of *Cruziana petraea* in the upper part of the Lower Sandstones of the Kufrah Basin (Lüning et al., 1999), an ichnospecies generally characterizing Middle to Upper Ordovician deposits that is also reported from Chad (Seilacher, 2007), we suggest the following attributions for the pre-glacial Lower Sandstones units on the basis of the recognition of two large transgressive cycles, which we acknowledge as two large Ordovician retrogradations over the platform.

- Unit 1: mostly Lower Ordovician sandstones, which should correspond to the proximal counterpart of sandstones recurrently showing *Cruziana* tracks of the Rugosa group more to the west and north. The lowermost shallow-marine segment might be the only representative, if any, of an (upper?) Cambrian sedimentation, though an earliest Ordovician age if favored.
- Unit 3: upper Lower to Middle Ordovician sandstones, which we correlate with the Floian to Darriwilian retrogradation recorded to the west (In Tahouite Fm. of Algeria; Hawaz Fm. of Libya). The overall 'transgressive' trend is highlighted by conditions favorable to a *Cruziana* ichnofacies development at the top of Unit 3.

An alternative correlation might have considered that the two transgressive wedges relate to Early-Middle (Unit1) and Late (Unit 3) Ordovician cycles; the latter being well known for a major retrogradation over north and west Africa (Gatinskiy et al., 1960; Kichou-Braîk et al., 2006) and the Middle East (MFS O40 of Sharland et al., 2004). Upper Ordovician strata are, however, most often truncated by the end-Ordovician glacial erosion surfaces, except in the more distal segments of the platform (Ghienne et al., 2010) or in interfluve areas beneath the end-Ordovician glacial erosion surfaces (Bataller et al., 2019; Gil-Ortiz et al., 2022). Though these alternative attributions cannot be excluded, the change in paleocurrent trends noted from Unit 1 to Unit 3 (Fig. 4) is reminiscent of the change in drainage patterns that occurred in an Early to Middle Ordovician time interval (Beuf et al., 1971), favoring the Early to Middle Ordovician age attribution considering the Lower Sandstones of the Ennedi.

The status of the intervening Unit 2 is puzzling. It might be understood as an ultimate short-term 'parasequence' concluding the long-term transgressive stacking pattern initiated with Unit 1 and truncated by Unit 3, which represents an overlying transgressive wedge similar to Unit 1. This interpretation would suggest the Unit3/Unit 2 contact corresponds to a relatively long stratigraphic hiatus, which should correspond to the development of highstand to lowstand conditions in more distal areas. It however does not conform to large-scale loading structures underlining the contact, which indicate still non-lithified shales when the overlying sandstones were deposited. Another possibility would be to suggest a flooding linked to a short-term, but significant regressive-transgressive interval, for instance to a

glacio-eustatic event during the Early Ordovician. Going further, we note that the sequence of events linked to Unit 2 echoes the end-Ordovician development involving a glacio-isostatic flexure that allowed seawater to invade such a proximal area (see below). The Lower Ordovician inferred glaciers would have reached or at least been close to the Ennedi area. Although it required confirmation, this interpretation would explain well why the horizon of offshore shales characterizing the Unit 2 has been taken for a Lower Silurian interval by some previous geologists.

Whatever the age within the Ordovician, the proposed correlation framework depicts an overall south- to southeastward-oriented, continent-scale, progressive encroachment of the Lower Palaeozoic strata. It assumes the non-deposition and progressive disappearance of Middle-Upper Cambrian strata to the south and east, though correlative strata are well expressed to the north (northern Libya, north-Saharan basins of Algeria). The relatively monotonous coastal deposits preserved in the proximal reaches of the platform (Niger, SE Libya, Chad) are interpreted essentially as correlatives of transgressive Ordovician fine-grained inner-shelf to condensed successions in the north or NNW. Similar coastal suites are identified around Gondwana. In Jordan, they characterize an older upper Cambrian to Lower Ordovician interval (Disi Fm. Ghienne et al., 2010; Meischner et al., 2020), a time range logically expected in this intermediate, i.e., less proximal segment of the platform. In South Africa, the Peninsula Sandstone (Turner et al., 2011) is assigned to a time interval comparable to that of the Lower Sandstones of the Ennedi. Interestingly, the Peninsula Sandstone characterizes a proximal setting where the succession wedge-out onto basement rocks at the scale of a few tens of km, as should also occurred to the south of the Ennedi. Note that the relatively limited thickness (< 200 m) of the Ordovician in the study area might not be solely a signature of the proximality of the Ennedi, as along-strike thickness changes reflecting subsidence/uplift trends controlled by basement heterogeneities (Nkono et al., 2018) could also have played a significant role, as recognized elsewhere throughout the platform (Klitzsch, 1970; Perron et al., 2021).

6.2. *The end-Ordovician glacial record*

The basal erosion surface and conglomerates of Unit 4, as well as the exhumed overlying glacial erosion surface and glaciomarine deposits at the base of Unit 5, allow both units to be interpreted as representatives of the end-Ordovician glacial record. Unit 4 (Wadi Djoua Fm.) appears as the diachronous(?) proximal counterpart of the Mamuniyat Fm. of the Kufrah Basin (Le Heron et al., 2010; Le Heron and Howard, 2012). A “channelised unconformity” and an “intra-Mamuniyat unconformity” in the Jebel Azbah area of the eastern Kufrah Basin might correlated with the basal bounding surfaces of Unit 4 and Unit 5, respectively.

The preservation of the glacial record is restricted to glacially-cut overdeepenings, possibly palaeovalleys, flanked by less eroded interfluve areas, where Silurian-Devonian sandstones directly superimposed the preglacial Ordovician sandstones. The contrast between Unit 4 and Unit 5 is striking, the former dominated by conglomerate-prone outwash deposits, the latter being mainly a fine-grained subaqueous succession. Fining-up outwash deposits of Unit 4 suggest limited interferences with glacio-isostatic patterns during this earlier deglaciation phase, which is surprising in such a proximal setting. This might have been the case, however, if Unit 4 was principally deposited in the forefield of an ice sheet of a lesser

extent (a less extensive glacial maximum? or a major stabilization? see discussion in Girard et al., 2015). Fine-grained sedimentation of Unit 5 is more easily understandable as a consequence of a rapid ice-front retreat and deposition in a relatively and temporarily deep setting, both accounting for a major glacio-isostatic deflection in tens to hundreds of meters that inevitably interfered at that time with glacio-eustacy (Dietrich et al., 2019). The fine-grained sandstone interval within Unit 5 might relate in one way or another to the late glacial recurrence identified on the eastern side of the Tibesti, which occurred before the deposition of Rhuddanian 'warm' shales (Le Heron et al., 2015; Meinhold et al., 2016), which in turn can correlated with the uppermost shale interval of Unit 5.

The temporal framework of the Bedo Fm. (Unit 5) has to be further discussed. The occurrence in the same stratigraphic position of an uppermost Ordovician to lowermost Silurian fauna at *c.* 500 km to the NNW (Le Hérissé et al., 2013; Page et al., 2013) and *c.* 650 km to the NNE (Thusu et al., 2013) suggests the Unit 5 might be as older, or even slightly older — i.e., strictly latest Ordovician. The corresponding more distal deposits in the Kufrah Basin show well-developed more proximal HCS sandstone beds and a regressive evolution (Gindre et al., 2012; Le Heron et al., 2015) lacking in the Ennedi record. A latest Ordovician post-glacial, glacio-isostatically driven forced regression in the Ennedi area, with a coeval condensation to the north (or NW) might explain the distinct records. Such a setting predated the overall, long-term progradational trend characterizing the Lower Silurian (Bellini and Massa, 1980; Gindre et al., 2012). Therefore, the Bedo Fm. and Libyan analogues would be older than the Lower Silurian Tanezzuft shales usually defined in the Murzuq Basin (Bellini and Massa, 1980; Grignani et al., 1991; Le Hérissé et al., 2013; Lüning et al., 1999), as are similar records preserved in southeastern Algeria and northern Niger (Denis et al., 2010; Legrand, 2002).

The Lower Sandstones of the Ennedi is suggested to be essentially Ordovician in age. Here, the Palaeozoic succession illustrates the depositional conditions that occurred across one the most proximal segment of the north-facing Gondwana platform. It shows in particular that the Ordovician transgressions, well-characterized in North Africa (Ghienne et al., 2007), must have reached northern Chad. This archive also expands the area of glacially-controlled deposition to the south and east with respect to the pre-existing dataset. It confirms the eastward prolongation of the North African palaeoglacial framework in the eastern Sahara and, most likely, up to eastern Arabia and Ethiopia (Le Heron and Howard, 2012). As far south as the Ennedi, glaciomarine sedimentation and northward-flowing ice flows are recognized. It indicates Ordovician ice-divide areas positioned in southern Chad or even further to the south in Central Africa. Here, a glacial record of unknown age but displaying northward-oriented dispersal patterns is identified (Censier and Lang, 1992), which might correlate with the Chadian Ordovician record. A potential end-Ordovician record have also been inferred in Cameroon, where an undated ice-flow pattern toward the WSW has been documented (Caron et al., 2011). Disparate orientations would not be a real problem because opposite flow orientations might characterize a same glacial event in areas corresponding to former ice divides (Rice et al., 2020).

Acknowledgements : The authors wish to thank the Governor of the Ennedi-Ouest and the Prefect of Fada, as well as the staff of the Ennedi African Park for their hospitality and for facilitating the fieldwork. They also gratefully acknowledge the University of N'Djaména, the CNRD (Centre National de Recherche pour le Développement), and the French Embassy in N'Djaména for their financial and technical support. The authors are grateful to G. Meinhold and J.-N. Proust for their careful reviews, which helped improve an earlier version of the manuscript.

References

Anfray, R., Rubino, J.-L., 2003. Shelf depositional systems of the Ordovician Hawaz Formation in the central Al Qarqaf High. In : Salem, M. J., Oun, K. M., Seddiq, H. M. (Eds.), The Geology of Northwest Libya II, Vol. 3, Second Symposium on the Sedimentary Basin of Libya, Tripoli, Libya, vol. 3, pp. 123–134.

Aubineau, J., El Albani, A., Chi Fru, E., Gingras, M., Batonneau, et al., 2018. Unusual microbial mat- related structural diversity 2.1 billion years ago and implications for the Francevillian biota. Geobiology 16, 476-497.

Bataller, F. J., McDougall, N., Moscariello, A., 2019. Ordovician glacial paleogeography: Integration of seismic spectral decomposition, well sedimentological data, and glacial modern analogs in the Murzuq Basin, Libya. Interpretation 7, T383-T408.

Bellini, E., Massa, D., 1980. A stratigraphic contribution to the Palaeozoic of Southern basins of Libya. In : Salem, M. J., Busrewil, M. T. (Eds.), The Geology of Libya, Vol. I, Academic Press, London, pp. 3-56.

Beuf, S., Biju-Duval, B., De Charpal, O., Rognon, P., Gariel, O., Bennacef, A., 1971. Les grès du Paleozoïque inférieur au Sahara. Science et Technique du Pétrole 18, Paris, 465 p.

Bizard, C., Bonnet, A., Freulon, J.-M., Gerard, G., De Lapparent, A., Vincent, P., Wacrenier, P., 1955. La série géologique entre le Djado et le Tibesti (Sahara oriental). C.R. Acad. Sci. Paris 241, 1320-1323.

Bonnet, A., Freulon, J.-M., de Lapparent A.-F., Vincent P., 1955. Observations géologiques sur l'ennedi, le Mourdi et les Erdi (Territoire du Tchad, A.E.F.). C. R. Acad. Sci. Paris 241, 1403-1405.

BRGM, 2004.Carte offerte à l'occasion du 20ème Colloque de Géologie Africaine (Orléeans, June 2004). BRGM Editions, Orléans.

Buatois, L. A., Mángano, M. G., 2011. Ichnology: Organism-substrate interactions in space and time. Cambridge University Press, 357 p.

Caron, V., Mahieux, G., Ekomane, E., Moussango, P., Babinski, M., 2010. One, two or no record of late neoproterozoic glaciation in South-East Cameroon. J. Afr. Earth Sci. 59, 111-124.

Censier, C., Lang, J., 1992. La Formation glaciaire de la Mambéré (République Centrafricaine): Reconstitution paléogéographique et implications à l'échelle du Paléozoique africain. Geol. Rund. 81, 769-789.

Dabard, M. P., Loi, A., Paris, F., Ghienne, J.-F., Pistis, M., Vidal, M., 2015. Sea-level curve for the Middle to early Late Ordovician in the Armorican Massif (western France): Icehouse third-order glacio-eustatic cycles. Palaeogeog. Palaeoclim. Palaeoeco. 436, 96-111.

Dashtgard, S. E., Gingras, M. K., MacEachern, J. A., 2009. Tidally modulated shorefaces. J. of Sediment. Res. 79, 793-807.

De Lestang, J., 1965. Das Paläozoikum am Rande des Afro-Arabischen Gondwanakontinents. Z. deutsch. Geol. Ges. 117, 479-488.

Denaeyer M.-E., 1924. L'Ouadaï oriental et les régionsd voisines. Géographie physique, géologie, lithologie, d'après les documents de la mission de délimitation Ouadaï-Darfour. Bull. Soc. Géol. France 24, 538-576.

Denis, M., Guiraud, M., Konaté, M., Buoncristiani, J.-F., 2010. Subglacial deformation and water-pressure cycles as a key for understanding ice stream dynamics: evidence from the Late Ordovician succession of the Djado Basin (Niger). Intern. J. Earth Sci. 99, 1399-1425.
Deschamps, R., Eschard, R., Roussé, S., 2013. Architecture of Late Ordovician glacial valleys in the Tassili N'Ajjer area (Algeria). Sediment. Geol. 289, 124-147.
Deynoux, M., Sougy, J., Trompette, R., 1985. Lower Palaeozoic rocks of west Africa and the western part of central Africa. In : Holland, C. H. (Ed.), Lower Palaeozoic of north-western and west-central Africa, John Wiley & Sons, Chichester, pp. 337-495.
Dietrich, P., Ghienne, J. F., Lajeunesse, P., Normandeau, A., Deschamps, R., Razin, P., 2019. Deglacial sequences and glacio-isostatic adjustment: Quaternary compared with Ordovician glaciations. Geol. Soc. London, Spec. Publ. 475, 149-179.
Elicki, O., Altumi, M. M., 2019. Cambrian trace fossils from North Africa and their contribution to Gondwana's paleobiogeography and depositional history. J. Afr. Earth Sci. 158, article n° 103556.
Eschard, R., Braik, F., Bekkouche, D., Rahuma, M. B., Desaubliaux, G., Deschamps, R., Proust, J. N., 2010. Palaeohighs: their influence on the North African Palaeozoic petroleum systems. In : Petroleum Geology Conference series, Vol. 7, Geological Society, London, pp. 707-724.
Eyles, N., Putkinen, N., Sookhan, S., Arbelaez-Moreno, L., 2016. Erosional origin of drumlins and megaridges. Sediment. Geol. 338, 2-23.
Fabre, J., Kazi-Tani, N., 2005. Ordovicien, Silurien, Devonien, Permo-Carbonifère. In : Fabre, J. (Ed.), Géologie du Sahara occidental et central, Tervuren African Geoscience Collection, 18, Musée Royal de l'Afrique Centrale, Tervuren, Belgique. pp. 147-360.
Fritel, P.-H., 1924. Sur les restes de végétaux fossiles paléozoïques recueillis en Ouadaï par la mission du L^{t}-Col. Grossard. Bull. Mus. Hist. Nat. 1, 117-118.
Fritel, P-H., 1925. Végétaux paléozoïques et organismes problémafiques de l'Ouadaï. Bull. Soc. Géol. France 25, 33-48.
Gatinskiy, G., Klochko, V.P., Rozman, K.S., Trofimov, D.M., 1966. Nouvelles données sur la stratigraphie des dépôts paléozoïques du Sahara méridional. Doklady Akademii Nauk SSSR 170, 1154-1157.
Germann, K., Wipki, M., Schwarz, T., 1993. Cambro-Ordovician bauxitic laterites of NW-Sudan. In : Thorweihe, U., Schandelmeier, H. (Eds), Geoscientific Research in Northeastern Africa, Balkema, Amsterdam, pp. 335-340.
Ghienne, J.-F., Boumendjel, K., Paris, F., Videt, B., Racheboeuf, P., Ait Salem H., 2007. The Cambrian-Ordovician succession in the Ougarta Range (western Algeria, North Africa) and interference of the Late Ordovician glaciation on the development of the Lower Palaeozoic transgression on northern Gondwana. Bull. Geosc. 82(3), 183-214.
Ghienne, J.-F., Monod, O., Kozlu, H., Dean, W.T., 2010. Cambrian-Ordovician depositional sequences in the Middle East : a perspective from Turkey. Earth Sci. Rev. 101, 101-146.
Gil-Ortiz, M., McDougall, N. D., Cabello, P., Marzo, M., Ramos, E., 2022. Sedimentary architecture of a Middle Ordovician embayment in the Murzuq Basin (Libya). Mar. Petrol. Geol. 135, 105339.

Gindre, L., Le Heron, D., & Bjørnseth, H.M., 2012. High resolution facies analysis and sequence stratigraphy of the Siluro-Devonian succession of Al Kufrah basin (SE Libya). J. Afr. Earth Sci., 76, 8-26.
Girard, F., Ghienne, J.-F., Du-Bernard, X., Rubino, J.-L., 2015. Sedimentary imprints of former ice-sheet margins: Insights from an end-Ordovician archive (SW Libya). Earth-Sci. Rev. 148, 259-289.
Greiger, J., Pougnet, R., 1967. Essai de description des formations géologiques de la République du Niger. Direction des Mines et de la Géologie 3 (République du Niger). BRGM Ed., Paris, France
Grigagni, D., Lanzoni, E., Elatrash, H., 1991. Palaeozoic and Mesozoic subsurface palynostratigraphy in the Al Kufrah Basin, Libya. In : Salem, M. J., Hammuda, O. S., Eliagoubi, B. A. (Eds), The Geology of Libya, Vol. IV, Elsevier, Amsterdam, pp. 1160-1227.
Hart, B. S., Plint, A. G, 1995. Gravelly shoreface and beachface deposits. Spec. Publ. Int. Ass. Sediment. 22, 75-99.
Joulia, F. 1959. Les series primaires au N et NW de l'Aïr (Sahara central). Discordances observées. Bull. Soc. Géol. France 7, 192-196.
Kichou-Braîk, F., Samar, L., Fekirine, B., Legrand, P., 2006. Découverte de graptolites d'âge caradocien dans quelques sondages du Tinrhert (Sahara algérien). C. R. Palevol 5, 675-683.
Kilian, C., 1924. Notes sur la géologie du Sahara central. Trav. Lab. Géol. Fac. Sc. Univ. Grenoble 13, 87-102.
Klitzsch, E., 1965. Comments on the Geology of the central parts of Southern Libya and Northern Chad. Petroleum Exploration Society of Libya (Tripoli) 8, 1-17.
Klitzsch, E., 1968. Die Gotlandium-Transgression in der Zentral-Sahara. Z. deutsch. Geol. Ges. 117, 492-501.
Klitzsch, E., 1970. Die Strukturgeschichte der Zentralsahara. Geol. Rund. 59, 459-527.
Klitzsch, E., 1994. Geological exploration history of the Eastern Sahara. Geol. Rund. 83, 475-483.
Klitzsch, E., Reynolds, P.-O., Barazi, N., 1993. Geologische Erkundungsfahrt zum Ostteil des Ennedi Gebirges und der Mourdiu Depression (NE Sudan) im Januar 1992. Würzburger Geogr. Arbeiten 87, 49-61.
Lacroix, A., Tilho, J., 1919. Esquisse géologique du Tibesti, du Borkou, de l'Erdi et de l'Ennedi — Les formations sédimentaires. C.R. Acad. Sc., Paris 168, 1169-1174.
Lang, J., Le Heron, D. P., Van den Berg, J. H., Winsemann, J., 2021. Bedforms and sedimentary structures related to supercritical flows in glacigenic settings. Sedimentology 68, 1539-1579.
Le Hérissé, A., Paris, F., Steemans, P., 2013. Late Ordovician-earliest Silurian palynomorphs from northern Chad and correlation with contemporaneous deposits of southeastern Libya. Bull. Geosci. 83, 483-504.
Le Heron, D. P., 2018. An exhumed Paleozoic glacial landscape in Chad. Geology 46, 91-94.
Le Heron, D. P., Howard, J. P., 2012. Sandstones, glaciers, burrows and transgressions: the lower Palaeozoic of Jabel az-Zalmah, Al Kufrah basin, Libya. Sediment. Geol. 245, 63-75.
Le Heron, D. P., Sutcliffe, O. E., Whittington, R. J., Craig, J., 2005. The origins of glacially related soft-sediment deformation structures in Upper Ordovician glaciogenic rocks: implication for ice-sheet dynamics. Palaeogeog. Palaeoclim. Palaeoeco. 218, 75-103.

Le Heron, D.P., Armstrong, H.A., Wilson, C., Howard, J.P., Gindre, L., 2010. Glaciation and deglaciation of the Libyan Desert: The Late Ordovician record. Sediment. Geol. 223, 100-125.
Le Heron, D. P., Meinhold, G., Elgadry, M., Abutarruma, Y., Boote, D., 2015. Early Palaeozoic evolution of Libya: perspectives from Jabal Eghei with implications for hydrocarbon exploration in Al Kufrah Basin. Basin Res. 27, 60-83.
Le Heron D.P., Busfield M.E., Chen X., Corkeron M., Davies B.J., Dietrich P., Ghienne J.-F., Kettler C., Scharfenberg L., Vandyk T.M., Wohlschägl R. 2022 – New perspectives on glacial geomorphology in Earth's deep time record. Frontiers Earth Sci. 10, article n° 870359.
Leckie, D., 1988. Wave-formed, coarse-grained ripples and their relationship to hummocky cross-stratification. J. Sediment. Res. 58, 607-622
Legrand, P., 1974. Essai sur la paléogéographie de l'Ordovicien au Sahara algérien. Notes et Mémoires, Compagnie française des pétroles 11, 121-138.
Legrand, P., 2002. Bâtir une stratigraphie: les leçons de l'étude du Paléozoïque au Sahara algérien. Comptes Rendus Palevol 1, 383-397.
Lemoigne, Y., Durante, M., Blanc, C., 1992. Flores d'âge Carbonifère Inférieur du Niger et du Tchad. Geobios 25, 449-455.
Lessertisseur, J., 1956. Sur un bilobite nouveau du Gothlandien de l'Ennedi (Tchad, A.E.F.), *Cruziana ancora*. Bull. Soc. Géol. France 6, 43-47.
Liégeois, J.-P., Abdelsalam, M. G., Ennih, N., Ouabadi, A., 2013. Metacraton: nature, genesis and behavior. Gondwana. Res. 23, 220-237.
Lucchi, R. G., Sagnotti, L., Camerlenghi, A., Macrì, P., Rebesco, M., Pedrosa, M. T., Giorgetti, G., 2015. Marine sedimentary record of Meltwater Pulse 1a along the NW Barents Sea continental margin. Arktos 1, article n° 7.
Lüning, S., Craig, J., Fitches, B., Mayouf, J., Busrewil, A., El Dieb, M. et al., 1999. Re-evaluation of the petroleum potential of the Kufra Basin (SE Libya, NE Chad): does the source rock barrier fall? Mar. Petrol. Geol. 16, 693-718.
Lüning, S., Miles, N., Pearce, T., Brooker, E., Barnard, P., Johannson, G., Schäfer, S., 2010. Biostratigraphy, chemostratigraphy and thermal maturity of the A1-NC198 exploration well in the Kufra Basin, SE Libya. In : Petroleum Geology Conference series Vol. 7, Geol. Soc., London, pp. 761-770.
MEH (Ministère de l'Élevage et de l'Hydraulique), 2015. Carte hydrogéologique de la République du Tchad au 1:200 000, Ouvrages et Ressources, feuille NE-34-10 Fada. UNITAR and SWISSTOPO, Genève and Wabern.
Meinhold, G., Le Heron, D. P., Elgadry, M., Abutarruma, Y., 2016. The search for 'hot shales' in the western Kufra Basin, Libya: geochemical and mineralogical characterisation of outcrops, and insights into latest Ordovician climate. Arab. J. Geosci. 9, article n°62.
Meischner, T., Elicki, O., Masri, A., Moumani, K. A., Hussein, M. A. A., 2020. Ordovician trace fossils from southern Jordan with particular consideration to the Cruziana rugosa group: Taxonomy, stratigraphy and trans-regional correlation throughout the Middle East and northern Africa. J. Afr. Earth Sci. 164, article n° 103595.
Moreau, J., Ghienne, J.-F., Le Heron, D., Rubino, J.-L., Deynoux, M., 2005. A 440 Ma old ice stream in North Africa. Geology 33, 753-756.

Newton, A. M., Huuse, M., 2017. Glacial geomorphology of the central Barents Sea: Implications for the dynamic deglaciation of the Barents Sea Ice Sheet. Mar. Geol. 387, 114-131.
Nkono, C., Liégeois, J. P., Demaiffe, D., 2018. Relationships between structural lineaments and Cenozoic volcanism, Tibesti swell, Saharan metacraton. J. Afr. Earth Sci. 145, 274-283.
Page, A., Meinhold, G., Le Heron, D. P., Elgadry, M., 2013. *Normalograptus kufraensis*, a new species of graptolite from the western margin of the Kufra Basin, Libya. Geol. Mag. 150, 743-755.
Perron, P., Guiraud, M., Vennin, E., Moretti, I., Portier, E., Le Pourhiet, L., Konaté, M., 2018. Influence of basement heterogeneity on the architecture of low subsidence rate Paleozoic intracratonic basins (Reggane, Ahnet, Mouydir and Illizi basins, Hoggar Massif). Solid Earth 9, 1239-1275.
Perron, P., Le Pourhiet, L., Guiraud, M., Vennin, E., Moretti, I., Portier, É., Konaté, M. 2021. Control of inherited accreted lithospheric heterogeneity on the architecture and the low, long-term subsidence rate of intracratonic basins. BSGF-Earth Sci. Bull. 192, 15.
Proust, J. N., Pouderoux, H., Ando, H., Hesselbo, S. P., Hodgson, D. M. et al., 2018. Facies architecture of Miocene subaqueous clinothems of the New Jersey passive margin: Results from IODP-ICDP Expedition 313. Geosphere 14, 1564-1591.
Ravier, E., Buoncristiani, J. F., 2018. Glaciohydrogeology. In : Past glacial environments (second edition), Elsevier Ltd, pp. 431-466.
Rice, J. M., Ross, M., Paulen, R. C., Kelley, S. E., Briner, J. P., 2020. A GIS- based multi- proxy analysis of the evolution of subglacial dynamics of the Quebec–Labrador ice dome, northeastern Quebec, Canada. Earth Surf. Proc. Land. 45, 3155-3177.
Richet, P. and De Charpal, O., 1998. An example of platform sedimentation: the Saharan Cambro-Ordovician. In : Majithia, M. (ed.) Dynamics and Methods of Study of Sedimentary Basins, Editions Technip – Association des sédimentologistes français, 91–110 (translation of Dynamique et méthodes d'étude des bassins sédimentaires, 1989, Ed. Allen G.P.)
Rubino, J.-L., Anfray, R., Blanpied, C., Ghienne, J.-F., Manatschal, G., 2003. Meander belt complex within the lower Mamuniyat Formation in western Al Qarqaf area, Libya. In : Salem, M. J., Khaled Oun, M. (Eds), The Geology of Northwest Libya, Vol. II, Gutenberg Press, Malta, pp.3-18.
Rüther, D. C., Bjarnadóttir, L. R., Junttila, J., Husum, K., Rasmussen, T. L., Lucchi, R. G., Andreassen, K., 2012. Pattern and timing of the northwestern B arents S ea I ce S heet deglaciation and indications of episodic Holocene deposition. Boreas 4, 494-512.
Sandford, K. S., 1935. Geological Observations on the Northwest Frontiers of the Anglo-Egyptian Sudan and the adjoining part of the Southern Libyan Desert. Quart. J. Geol. Soc. 91, 323-381.
Schneider, J.-L., Wolff, J.-P., 1992. Carte Géologique et Carte Hydrogéologique 1/1500000 de la République du Tchad, Mémoire Explicatif. Documents du BRGM n° 209, Edition BRGM, Orléans, France, 531 p.
Seilacher, A., 1970. Cruziana stratigraphy of 'non-fossiliferous' Paleozoic sandstones. In : Crimes, T. P., Harper, J. W. (Eds.), Trace Fossils, Geol. J. Special Issue, vol. 3., pp. 447–476.
Seilacher, A., 2007. Trace Fossil Analysis. Springer, Berlin, 226 p.

Seilacher, A., Lüning, S., Martin, M. A., Klitzsch, E., Khoja, A., Craig, J., 2002. Ichnostratigraphic correlation of lower Palaeozoic clastics in the Kufra Basin (SE Libya). Lethaia 35, 257-262.
Sharland, P. R., Casey, D. M., Davies, R. B., Simmons, M. D., Sutcliffe, O. E. (2001). Arabian plate sequence stratigraphy (GeoArabia Spec. Publication 2), Gulf PetroLink, Bahrain, 371 p.
Smith, J. A., Graham, A. G., Post, A. L., Hillenbrand, C. D., Bart, P. J., Powell, R. D., 2019. The marine geological imprint of Antarctic ice shelves. Nat. Comm. 10, article n°5635.
Spagnolo, M., Clark, C. D., Ely, J. C., Stokes, C. R., Anderson et al., 2014. Size, shape and spatial arrangement of mega- scale glacial lineations from a large and diverse dataset. Earth Surf. Proc. Land. 39, 1432-1448.
Thomas, K., Herminghaus, S., Porada, H., Goehring, L., 2013. Formation of Kinneyia via shear-induced instabilities in microbial mats. Philos. Trans. Royal Soc. A 371, article n° 20120362.
Thusu, B., Rasul, S., Paris, F., Meinhold, G., Howard, J. P., Abutarruma, Y., Whitham, A. G., 2013. Latest Ordovician–earliest Silurian acritarchs and chitinozoans from subsurface samples in Jebel Asba, Kufra Basin, SE Libya. Rev. Palaeobot. Palyno. 197, 90-118.
Trompette, R., 1983. Le Paléozoïque du Niger et du Tchad. In : Fabre J. (Ed.), West Africa, Geological Introduction and Stratigraphic Terms. Pergamon Press, Oxforf, pp. 121-126.
Turner, B. R., Armstrong, H. A., Holt, P., 2011. Visions of ice sheets in the early Ordovician greenhouse world: Evidence from the Peninsula Formation, Cape Peninsula, South Africa. Sediment. Geol. 236, 226-238.
Turner, B. R. 1980. Palaeozoic sedimentology of the southeastern part of Al Kufrah Basin, Libya: a model for oil exploration. In : Salem, M. J., Busrewil, M. T. (Eds), The Geology of Libya, Vol. II, Academic Press, London, 351-374.
Turner, B. R., 1991. Palaeozoic deltaic sedimentation in the southeastern part of Al Kufrah Basin, Libya. In : M. J. Salem, M.J., Belaid M. N. (Eds), The Geology of Libya, Vol. V, Elsevier, Amsterdam, pp. 1713-1726.
Wacrenier, P., 1958. Notice explicative de la carte géologique provisoire du Borkou- Ennedi-Tibesti au 1 : 1 000 000, Dir. des Mines et de la Géologie (AEF), Brazzaville, Congo, 24 p.
Wolff, J.-P., 1964. Carte Géologique de la République du Tchad, BRGM, Paris, France.
Zecchin, M., Catuneanu, O., Caffau, M., 2017. High-resolution sequence stratigraphy of clastic shelves V: criteria to discriminate between stratigraphic sequences and sedimentological cycles. Mar. Petrol. Geol. 85, 259-271.

Table 1. Coordinates of observation points where features 1-16 positioned in Fig. 4 were best observed. Coordinates of Fig. 6 and 5D are also given.

point	place names		latitude (N)	longitude (E)	related figure
1	Deli	gravelly-shoreface deposits	16°49.34’	21°27.24’	3A
2	Deli	piperock ichnofabric	16°49.30’	21°27.27’	3A
3	Bogaro	large-scale cross-stratification	16°04.88’	21°16.73’	3B, 5B
4	Bogaro	large-scale loading structure	16°04.94’	21°16.42’	
5	Bogaro	planar and through cross-stratification	16°05.00’	21°16.43’	5C
6	Hagoto	large gutters	17°18.85’	21°22.90’	
7	Hagoto	sand injections	17°16.55’	21°25.18’	
8	Wadi Torbo	intraformational grooves	17°20.60’	21°19.14’	
9	Fada pass	conglomerates and backsets	17°12.79’	21°26.06’	7E
10	Wadi Torbo	glacial lineations	17°19→22’	21°18→19’	3D, 7A-B-D
11	Wadi Torbo	sandstone-congl. bed, ripples on top	17°20.15’	21°18.78’	
12	Wadi Torbo	mud and granules (diamictite)	17°18.54’	21°21.06’	
13	Wadi Torbo	sandstone boulder (dropstone)	17°19.56’	21°19.16’	
14	Wadi Torbo	Kinneyia-like wrinkle marks	17°18.33’	21°21.03’	5E
15	Hagoto	wave megaripples & HCS	17°15.79’	21°27.08’	
16	Wadi Torbo	warm(?) shales	17°21.28’	21°19.88’	5F
	Hagoto	*Cruziana* and *Arthophycus*	17°18.95’	21°23.06’	5D
	Baki	large-scale through cross-stratification	~17°02.44’	21°16.58’	6 (upper)
	Hagoto	large-scale through cross-stratification	~17°19.08’	21°23.69’	6 (lower)